Runoff study on real terrains using UAV photogrammetry and SPH modelling of fluids.

A. Barreiro, J.M. Domínguez, A.J.C. Crespo, M. Gómez-Gesteira.

Environmental Physics Laboratory (EPHYSLAB), Universidade de Vigo, Spain.

H. González-Jorge

Applied Geotechnology Group. Department of Natural Resources & Environmental Engineering, Universidade de Vigo, Spain.

Keywords: SPH, numerical modelling, UAV, photogrammetry, runoff.

Abstract

Runoff problems due to intense rains can affect civil constructions causing instabilities in the terrain and even damages on structures. Two different technologies are merged to study this phenomena, UAV photogrammetry (Unmanned Air Vehicle) and a CFD model (Computational Fluid Dynamics) based on SPH (Smoothed Particle Hydrodynamics). UAV is used to obtain the topographic information about the area of study, and SPH technique is applied to study water trajectories in an extreme rain event. The use of engineering solutions to palliate flood events is also analysed.

1 Introduction

Surface runoff is the amount of water that soils cannot infiltrate. The source of the water can be snowmelt or intense rain events and can flow over the roads, the sidewalks, the roofs of the houses and any other impervious surface or soils.

The storms passing through the north of the Iberian Peninsula are frequently accompanied by heavy showers that result in short and intense rainfalls, in the order of 10-20 minutes. Due to climate change these events have worsened during the last decades and the area is more prone to extreme rain events than in the past. Therefore, civil structures must be prepared for the new conditions and need to be adapted to the new reality, where runoff can cause problems of stability of slopes, bridges, and walls.

Two advanced tools are combined in this work. UAV (Unmanned Air Vehicle) photogrammetry is used to obtain accurate topographic information of the area of study and the SPH (Smoothed Particle Hydrodynamics) code called DualSPHysics allows modelling complex flows.

UAV systems have become a new tool for remote acquisition of images. These devices can operate where traditional methods cannot, usually due to cost, danger issues or lack of flexibility. When UAVs are equipped with digital cameras, they become platforms that can provide useful topographic data, Remondio [1]. This tool represents a new alternative to the expensive LIDAR or photogrammetric traditional flights performed with a manned airplane. Other advantage of the UAV flights is the operational altitude, these devices can work at lower heights providing higher resolution, therefore, better accuracy Everaerts [2].

SPH is a meshless lagrangian method where the fluid is discretized by particles. Each particle represent a point where the main physical quantities are computed as the interpolation of the values of surrounding particles. The interaction is computed according to the Navier-Stokes equations, thus, density, pressure, and velocity of each particle are obtained.

The SPH code, DualSPHysics (Crespo [3], Gómez-Gesteira [4] [5]), has been developed to be applied to real engineering problems. The code can be run both on CPUs and GPUs (graphic processing units with powerful parallel computing capability). DualSPHysics is an open source project and can be download for free from www.dual.sphysics.org. The different details on the implementation can be found in Domínguez [6][7][8]. The model has been applied successfully to study different cases of civil engineering such as: computation of forces exerted by large waves on the urban furniture Barreiro [9] and run-up in an armour block breakwater Altomare [10].

In this work DualSPHysics is used to simulate the runoff on a terrain whose geometry was obtained using UAV photogrammetry. The case study represents how the water from an intense rain event flows into a road and how effective are the countermeasures implemented to palliate these kind of events. Thus a study of the different amount of water arriving to the road is carried out for different protection scenarios.

2 Methods

2.1 UAV technology

The UAV used in this study was an eight propeller Okto XL from Mikrokopter, for the detailed specifications the reader is referred to the website of the product (www.mikrokopter.de). The UAV is controlled by a remote station which tracks the position, velocity, and acceleration in the three axis, also other flight statistics are displayed such as pitch, roll, and relative height to the ground. The control station also uses the GPS signal to improve the UAV stability. The camera used for image acquisition is a Sony Nex 7 with a resolution of 24.3 Mpx. Mounted lens is a Sony SEL16F28 (focal length of 16 mm and F2.8).

Data acquisition was first planned in the laboratory using Google Earth and the Mikrokopter planning software to generate the GPS waypoints to configure the pathing of the survey, Figure 1.

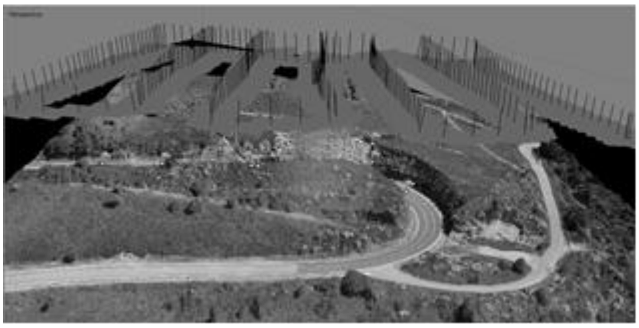

Figure 1: UAV pathing and image alignment with computed camera positions and the resulting point cloud.

The route, waypoints, and photography acquisition positions were configured to obtain a 60% image overlap. Once the flight was done autonomously by the UAV, the images obtained were loaded in a photogrammetric software called Photoscan (www.agisoft.ru). This software searches for the common points on the UAV photographs and places the points in the 3D space creating a point cloud with the geometric information as can be seen on Figure 1.

2.2 Smoothed Particle Hydrodynamics model

In this work only the main formulation of the SPH method is presented, for a deeper description of the method and its features the reader is referred to Gómez-Gesteira [4][5][11] and Monaghan [12].

As mentioned before SPH is a Lagrangian meshless method where de fluid is discretized as a set of particles. Each one of the particles is a nodal point where the main physical quantities are calculated (position, velocity, acceleration, density, pressure…). These quantities are computed as interpolation of the values of the neighbouring particles. The contribution of these particles is weighted using a kernel function (*W*). This function controls the contribution according to the distance between particles and its range of interaction is defined by the smoothing length (*h*). The smoothing length defines the maximum distance of interaction, meaning that particles with a bigger separation than *h* will not interact. The kernel function must satisfy certain properties like compact support, positivity, partition of unity and delta behaviour when the interaction distance tends to zero.

The SPH method is based in the integral interpolants theory, therefore any function, *F*, can be approximated by the integral:

$$F(\mathbf{r}) = \int F(\mathbf{r}')W(\mathbf{r}-\mathbf{r}',h)d\mathbf{r}' \qquad (1)$$

where **r** is the position vector of the particle, and *W* is the kernel function mentioned before.

There are many kernel functions in the literature but in DualSPHysics there are two options implemented, one of them is the Wendland quintic kernel by Wendland [13] defined in 3D as:

$$W(q) = \alpha_D \left(1-\frac{q}{2}\right)^4 (2q+1) \qquad 0 \le q \le 2 \qquad (2)$$

where $q=r/h$ and α_D = 21/(16πh3) is the normalization constant.

The function *F* (Eq. 1) can be expressed in a discrete form as:

$$F(\mathbf{r}_a) \approx \sum_b F(\mathbf{r}_b)W(\mathbf{r}_a-\mathbf{r}_b,h)\frac{m_b}{\rho_b} \qquad (3)$$

where *a* refers to the particle where the interpolation is taking place and *b* represents the neighbouring particles, also m and ρ are mass and density respectively.

The classical SPH formulation treats the fluid as weakly compressible and the Navier-Stokes equations are solved (Gómez-Gesteira [11].). The conservation laws of continuum fluid dynamics, in the form of differential equations, are transformed into their discrete forms by the use of the kernel functions.

The momentum equation was proposed by Monaghan [14] is used to determine the acceleration of a particle as the result of the interaction with its neighbours:

$$\frac{d\mathbf{v}_a}{dt} = -\sum_b m_b \left(\frac{P_b}{\rho_b^2} + \frac{P_a}{\rho_a^2} + \Pi_{ab} \right) \nabla_a W_{ab} + \mathbf{g} \qquad (4)$$

being **v** velocity, P pressure, ρ density, m mass, and **g** the gravitational acceleration. Π_{ab} is the viscous term according to the artificial viscosity proposed in Monaghan [12].

The mass of each particle is constant, so that changes in fluid density are computed by solving the conservation of mass or continuity equation in SPH form:

$$\frac{d\rho_a}{dt} = \sum_b m_b \mathbf{v}_{ab} \cdot \nabla_a W_{ab} \qquad (5)$$

The fluid is treated as weakly compressible, in this approach the pressure is calculated starting from density values of the particle using Tait's equation of state (Batchelor [15]).

3 Data pre-processing

The photogrammetric data is obtained as a point cloud with high resolution and the geometric information of the area. In order to perform the simulations is necessary to convert this data to a set of SPH particles. The steps taken are: first a conversion from *POINTS to TRIANGLES* then *TRIANGLES to SPH particles.*

3.1 POINTS to TRIANGLES

This process transforms the point cloud generated by Photoscan, Figure 2 left panel, to a polygon mesh using a 2D Delauny triangulation. Figure 2 centre panel. A mesh is a Delaunay triangulation if all circumcircles of all triangles of the network are empty. The generation of the mesh is crucial because it closes possible holes on the geometry and allows the realistic water displacement without abnormal infiltration. Therefore, a STL file can be produced, Figure 2 centre panel.

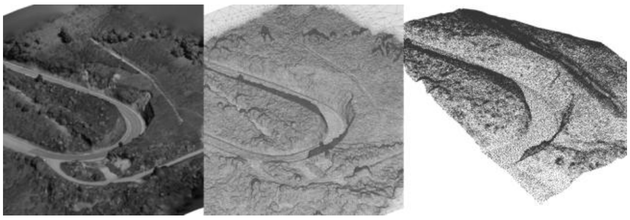

Figure 2: Stages of the data process from points to SPH particles.

3.2 TRIANGLES to SPH particles

DualSPHysics employs a pre-processing tool that uses a 3D mesh to locate the particles. The idea is to represent the objects using particles, these particles are created in the nodes of the 3D mesh. Firstly, the mesh nodes around the object are defined and then particles are created only in the nodes that compose the shape of the desired geometry. Complex 3D models such as STL files can be imported and converted to particles, Figure 2 right panel, splitting the geometry into triangles and following the process described before.

4 Case of study

Figures 1 and 2 present the case of study. The road section studied is located around 42.2946°N and 7.5888° W. Rain causes important damages that can be observed in the surrounding orography. These kind of events motivates this work. The slopes of the road are mainly formed by shale that is a natural waterproofing rock, thereby, the amount of water infiltrated is minimum. The height of the slopes oscillates between 10 m and 15 m.

Figure 3 presents the domain of the simulation performed using DualSPHysics. The watermarked area on Figure 3 top, represents the catchment area that concentrates the water that will fall into the road. The watershed lower boundary corresponds to the upper boundary of the simulated area, darkened area on Figure 3 bottom.

Figure 3: Domain of the SPH simulation.

The area of study is 83 m x 75 m with a steep slope (~17%) in X direction and a gentler slope (~7%) in Y direction. The presence of a ditch across the terrain can also be observed in the figure, which is approximately 0.80 m deep and 0.5 m wide. The ditch is a temporary measure carved by an excavator. In order to appropriately represent the runoff inlet and outlet conditions are considered in the simulation frontiers. The lateral and lower boundaries are open so particles can freely exit the domain. In the other hand at the top frontier inflow conditions are imposed to mimic the effects of an intense rain event. The inflow conditions allows controlling the amount of water that enters the domain. The flow is calibrated to 0.5 m^3s^{-1}, the discharge is calculated according to the climatology and orography of the area, Pilgrim [16], for a deeper description of the process the reader is addressed to Barreiro [17]. Figure 4 presents the time story of the discharge that enters the domain and coincides with the expected value mentioned before.

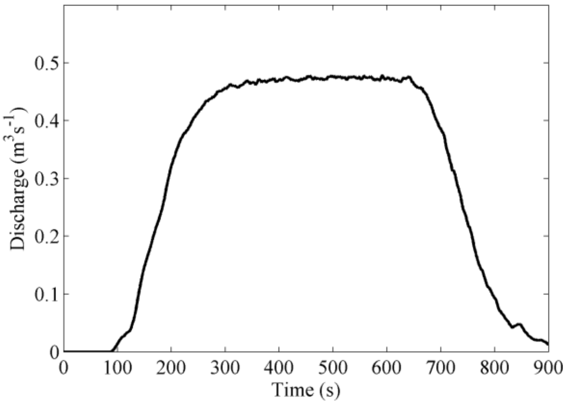

Figure 4: Time story of water inflow through the upper boundary.

The terrain is mostly filled with bushes creating a natural barrier to the flow advance. To represent this scenario a modification on DualSPHysics is necessary. The modification of the interaction between fluid and boundary particles allows the code imitating the behaviour of the flow interacting with vegetation. The coefficient of Manning characterizes a natural channel by the type of material or the amount of debris in it. Table 1 presents different values for the Manning coefficient.

Table 1. Typical table caption.

Surface	Value
Glass	0.010±0.002
Concrete	0.012±0.002
Steel	0.014±0.003
Natural channel	0.040±0.010
Area (low brush)	0.050±0.020
Area (high brush)	0.075±0.025

The Manning equation, Eq. 6, gives a theoretical velocity for a flow depending on the channel characteristics.

$$V = \frac{1}{n} R^{2/3} \sqrt{S} \tag{6}$$

where V is the theoretical velocity, n is the Manning coefficient, R is the hydraulic radius of the flow, and S the slope of the natural channel.

The modification of the interaction must be calibrated, so various simulations were carried out for different values of the interaction between fluid and boundary particles, α_{BF}/α_{FF}, Figure 5.

The Manning coefficient for high brush area is approximately 0.075, which results in a velocity of 0.46 ms^{-1}. According to Figure 5 the theoretical velocity was achieved for α_{FB}=16 α_{FF}.

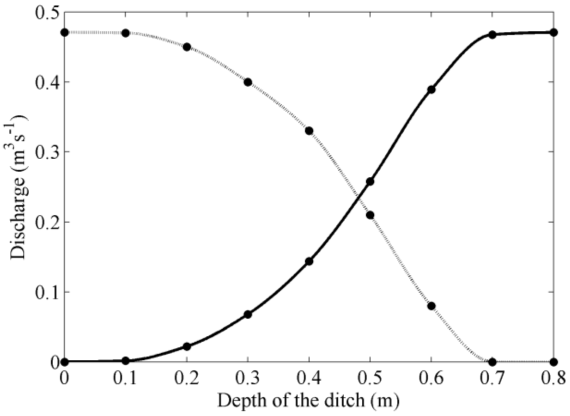

Figure 5: Flow velocity dependence on the ratio between α_{BF} and α_{FF}.

5 Results

The first simulation was conducted without the ditch, Figure 6, to evaluate the worst case scenario. The first two panels water only affects the upper (Time=100 s) and middle (Time=150 s) parts of the computational domain. In the third panel (Time=200 s) the water has already arrived at the lower part of the domain and falls into the road.

The amount of water arriving at the road can be seen in Figure 7. Basically, the plot is similar to the one showing the flow entering the computational domain (Figure 4). The maximum amount of water (around 0.46 m3s-1) is slightly smaller in Figure 7 because a small percentage of water (around 6%) leaves the computational domain through the open lateral boundaries. In addition, the signal in Figure 7

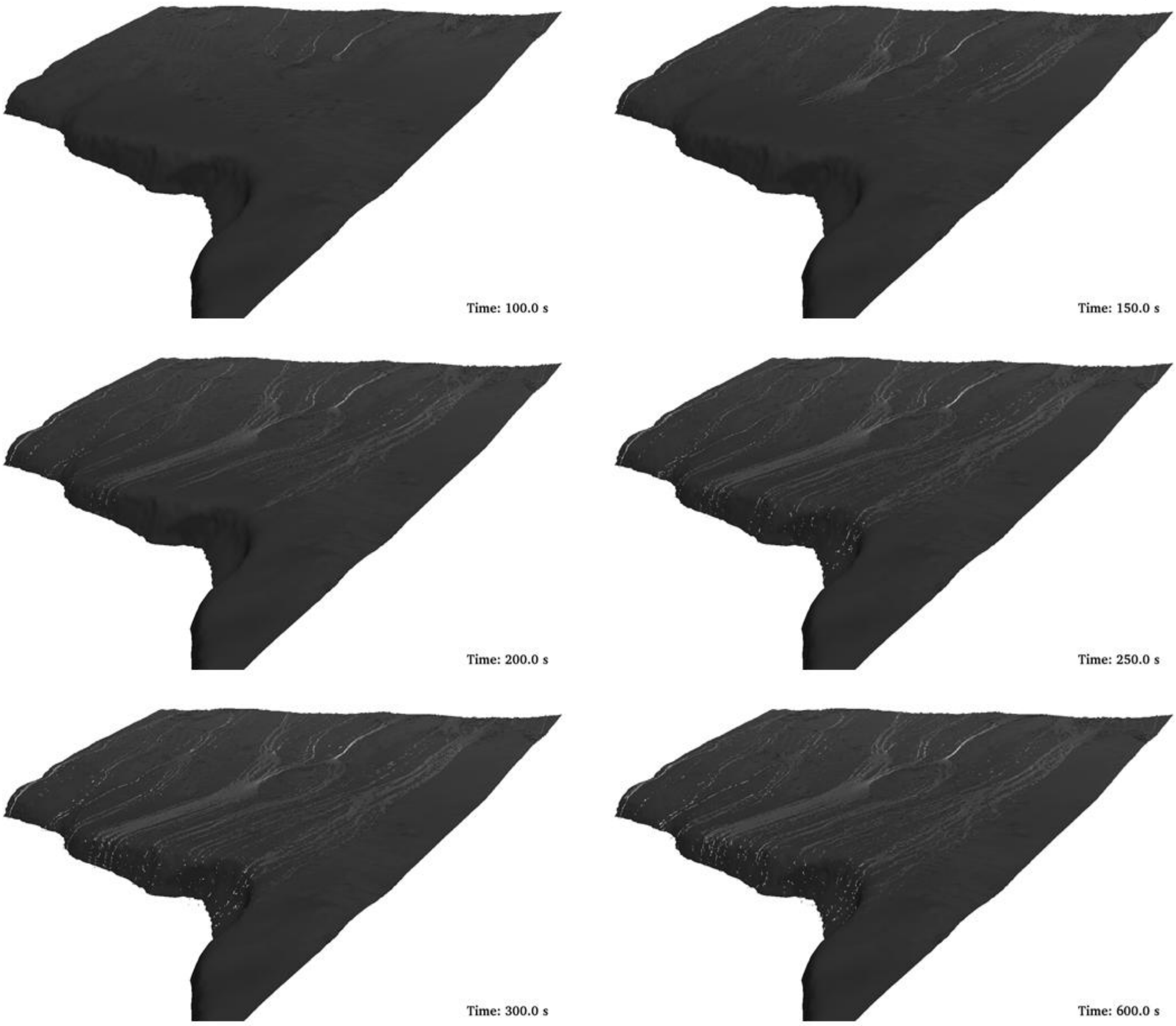

Figure 6: Different instants of the DualSPHysics simulation without ditch.

is delayed in around 50 seconds when compared with the signal in Figure 4.

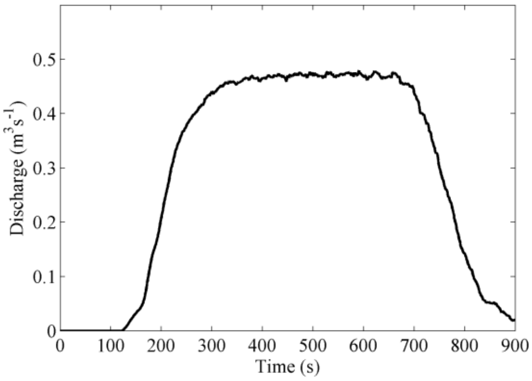

Figure 7: Time story of water inflow to the road.

A second simulation with the ditch was performed, Figure 8, the initial configuration of both cases is equal. The ditch mimics the main features of the real one shown in Figures 2 and 3; namely, 80 cm deep and 50 cm wide. The fist frames of the simulation are equal to previous simulation without a ditch. Nevertheless, the rest of the frames show how water is collected and drained by the ditch. Actually, there is not water discharge to the road under these conditions.

The ditch is temporary solution due to the degeneration of the carved area. This degeneration can be generated by debris or sedimentation caused by intense rain events. The effect of the sedimentation is analysed reducing the depth of the ditch. Figure 9 shows the water discharge into the road and the water drained by the ditch as a function of the depth of the ditch. The inflow conditions are the same as in previous cases. Ditches with less than 0.2 m are inefficient and 90% of the discharge arrives to the road. In the other hand ditches with around 0.4 m are able to drain the 50% of the incoming flow. Finally, ditches with more than 0.7 m depth are shown to be ideal draining the 100% of the discharge under strong rain conditions.

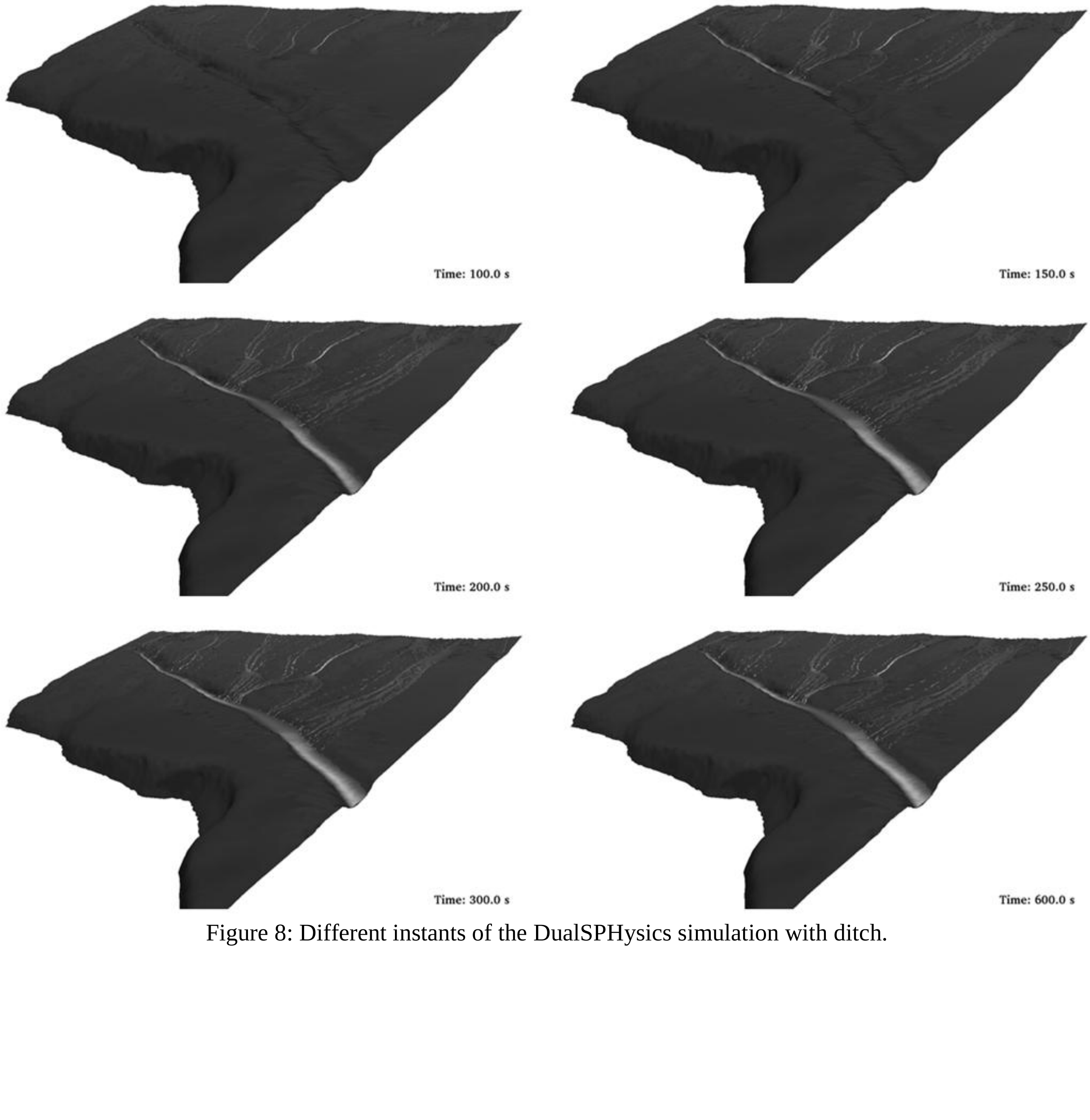

Figure 8: Different instants of the DualSPHysics simulation with ditch.

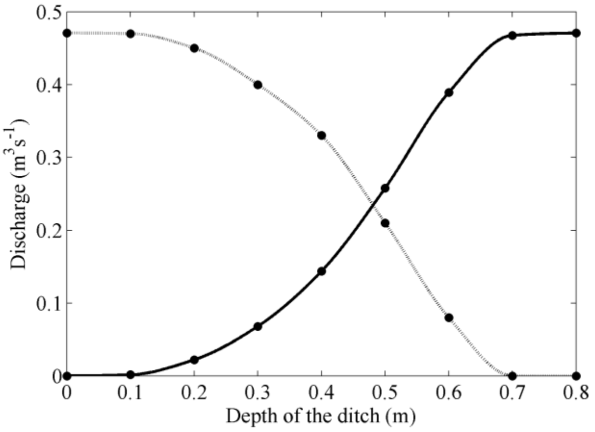

Figure 9: Discharge into the road (dashed line) and drainage of the ditch (solid line).

6 Conclusions

This work presents the combined application of two new technologies to study runoff problems on real terrains. These technologies are UAV photogrammetry and a fluid solver based on SPH technique.

UAV photogrammetry was used to obtain the geometry of the area. The point cloud data can be converted into particles through a triangulation process and these particles are used to create the initial setup of DualSPHysics.

The simulations use an inflow that mimics fast and intense rain events according to the meteorological conditions in the zone. Thus, an inflow of about 0.5 m^3s^{-1} was imposed through the upper boundary of the computational domain.

The effect of a ditch to prevent inflow to the road was studied. The dimensions of the ditch were 0.8 m deep and 0.5 m wide. This precautionary measure was observed to be effective to drain water under extreme conditions. Also a study for different ditch depths was conducted showing that the sedimentation decreases the efficiency. The drainage was only on the order of 50% when the depth of the ditch decreased at about 0.45 m.

In summary, the combination of UAV photogrammetry and DualSPHysics has proven to be a suitable tool to design measures to palliate floods on areas adjacent to roads. This method can be applied to any scenario.

References

[1] Fabio Remondino, L Barazzetti, Francesco Nex, Marco Scaioni & Daniele Sarazzi. UAV photogrammetry for mapping and 3D modelling- current status and future perspectives. Volume 38-1, page 25-31 International Archives of the Photogrammetry, Remote Sensing and Spatial Information Sciences. 2011.

[2] Jurgen Everaerts. The Use of Unmanned Aerial Vehicles (UAVS) for Remote Sensing and Mapping. IAPRS&SIS. 37(B1) (2008) 1187-1192.

[3] Alejandro J.C. Crespo, Jose M. Domínguez, Anxo Barreiro, Moncho Gómez-Gesteira & Benedict D. Rogers. GPUs, a new tool of acceleration in CFD: Efficiency and reliability on Smoothed Particle Hydrodynamics methods. PLoS ONE. 6(6) (2011) e20685

[4] Moncho Gómez-Gesteira, Benedict D. Rogers, Alejandro J.C. Crespo, Robert A. Dalrymple, Muthukumar Narayanaswamy & Jose M. Domínguez. SPHysics - development of a free-surface fluid solver- Part 1: Theory and Formulations. Computers & Geosciences. 48 (2012a) 289-299.

[5] Moncho Gómez-Gesteira, Alejandro J.C. Crespo, Benedict D. Rogers, Robert A. Dalrymple, Jose M. Domínguez & Anxo Barreiro. SPHysics - development of a free-surface fluid solver- Part 2: Efficiency and test cases. Computers & Geosciences. 48 (2012b) 300-307.

[6] Jose M. Domínguez, Alejandro J.C. Crespo, Moncho Gómez-Gesteira & Jean C. Marongiu. Neighbour lists in Smoothed Particle Hydrodynamics. International Journal For Numerical Methods in Fluids. 67(12) (2011) 2026-2042.

[7] Jose M. Domínguez, Alejandro J.C. Crespo & Moncho Gómez-Gesteira. Optimization strategies for CPU and GPU implementations of a smoothed particle hydrodynamics method. Computer Physics Communications, 184(3) (2013a) 617-627.

[8] Jose M. Domínguez, Alejandro J.C. Crespo, Benedict D. Rogers & Moncho Gómez-Gesteira. New multi-GPU implementation for Smoothed Particle Hydrodynamics on heterogeneous clusters. Computer Physics Communications, 184 (2013) 1848-1860.

[9] Anxo Barreiro, Alejandro J.C. Crespo, Jose M. Domínguez & Moncho Gómez-Gesteira. Smoothed Particle Hydrodynamics for coastal engineering problems. Computers & Structures, 120(15) (2013) 96-106.

[10] Corrado Altomare, Alejandro J.C. Crespo, Jose M. Domínguez, Xavier Gironella & Moncho Gómez-Gesteira. Numerical modelling of ar-

mour block sea breakwater with Smoothed Particle Hydrodynamics. Computers and Structures, 130 (2014) 34-45.

[11] Moncho Gómez-Gesteira, Benedict D. Rogers, Robert A. Dalrymple & Alejandro J.C. Crespo. State-of-the-art of classical SPH for free-surface flows. Journal of Hydraulic Research, 48 Extra Issue (2010) 6–27.

[12] Joseph J. Monaghan. Smoothed Particle Hydrodynamics, Reports on Progress in Physics. 68 (2005) 1703-1759.

[13] Holger Wendland. Piecewiese polynomial, positive definite and compactly supported radial functions of minimal degree. Advances in computational Mathematics, 4(1) (1995) 389-396.

[14] Joseph J. Monaghan. Smoothed Particle Hydrodynamics, Annual Rev. Astron. Appl. 30 (1992) 543-574.

[15] George K. Batchelor. Introduction to fluid dynamics, Cambridge University Press. 1974.

[16] David H. Pilgrim & Ian Cordery. Flood Runoff. Handbook of Hydrology, McGrawHill. 1993.

[17] Anxo Barreiro, Jose M. Domínguez, Alejandro J.C. Crespo, Higinio González-Jorge, David Roca & Moncho Gómez-Gesteira. Integration of UAV photogrammetry and SPH modelling of fluids to study runoff on real terrains. PLoS ONE, 9(11): e111031. 2014.